

## Fastigial nuclei surgical damage and focal midbrain disruption implicate PAG survival circuits in cerebellar mutism syndrome

Samuel S. McAfee<sup>®</sup>, Silu Zhang, Ping Zou, Heather M. Conklin, Darcy Raches, Giles Robinson, Amar Gajjar, Raja Khan, Paul Klimo, Zoltan Patay, and Matthew A. Scoggins

*Department of Diagnostic Imaging, St. Jude Children's Research Hospital, Memphis, Tennessee, USA (S.S.M., S.Z., P.Z., Z.P., M.A.S.); Department of Psychology, St. Jude Children's Research Hospital, Memphis, Tennessee, USA (H.M.C., D.R.); Department of Oncology, St. Jude Children's Research Hospital, Memphis, Tennessee, USA (G.R., A.G., R.K.); Department of Surgery, St. Jude Children's Research Hospital, Memphis, Tennessee, USA (P.K.); Department of Neurosurgery, University of Tennessee Health Science Center, Memphis, Tennessee, USA (P.K.); Le Bonheur Neuroscience Institute, Le Bonheur Children's Hospital, Memphis, Tennessee, USA (P.K.)*

**Corresponding Author:** Samuel S. McAfee, PhD, Department of Diagnostic Imaging, St. Jude Children's Research Hospital, 262 Danny Thomas Pl, Chili's Care Center, Room I3210, Memphis, TN 38105, USA ([stuart.mcafee@stjude.org](mailto:stuart.mcafee@stjude.org)).

### Abstract

**Background.** Pediatric postoperative cerebellar mutism syndrome (CMS) is a rare but well-known complication of medulloblastoma (Mb) resection with devastating effects on expressive language, mobility, cognition, and emotional regulation that diminishes quality of life for many Mb survivors. The specific anatomical and neuronal basis of CMS remains obscure. We address this issue by identifying patterns of surgical damage and secondary axonal degeneration in Mb survivors with CMS.

**Methods.** Children with Mb deemed high risk for CMS based on intraventricular location of the tumor had T1 images analyzed for location(s) of surgical damage using a specially developed algorithm. We used three complementary methods of spatial analysis to identify surgical damage linked to CMS diagnosis. Magnetization transfer ratio (MTR) images were analyzed for evidence of demyelination in anatomic regions downstream of the cerebellum, indicating neuronal dysfunction.

**Results.** Spatial analyses highlighted damage to the fastigial nuclei and their associated cerebellar cortices as the strongest predictors of CMS. CMS-related MTR decrease was greatest in the ventral periaqueductal gray (PAG) area and highly consistent in the left red nucleus.

**Conclusion.** Our evidence points to disruption of output from the fastigial nuclei as a likely causal trigger for CMS. We propose that core CMS symptoms result from a disruption in the triggering of survival behaviors regulated by the PAG, including the gating of vocalization and volitional movement. The fastigial nuclei provide the densest output to the PAG from the cerebellum, thus sparing these structures may provide a greater likelihood of CMS prevention.

### Key Points

- Damage to fastigial nuclei during medulloblastoma resection increases the risk of postoperative mutism.
- Mutism is linked to disruption of midbrain circuits tasked with the gating of speech production.

## Importance of the Study

Rates of postoperative mutism in high-risk medulloblastoma patients have hit a floor of about 25%-35% and failed to improve over the past decade. Systematic study of CMS pathogenesis has proven challenging due to the rarity of the disorder, the variability of symptoms accompanying mutism, and the lack of animal models for comprehensive study. Here, we examine patient data acquired over 10 years in a high-volume pediatric cancer center for what is, to the best of our

knowledge, the largest lesion-mapping study conducted in Mb patients deemed high risk for CMS. Importantly, the evidence presented here lends validity to the use of animal models to study vocal gating induced by the fastigial nuclei and PAG as a driver of mutism. Future research in animals will create a better understanding of how surgery leads to mutism for the purpose of prevention and could provide possible avenues for intervention in children already impacted by CMS.

Postoperative pediatric cerebellar mutism syndrome (CMS), also known as posterior fossa syndrome (PFS), is a disorder seen in some patients after surgical resection of posterior fossa tumors, most commonly for midline, intraventricular medulloblastoma (Mb). While not typically evident immediately after surgery, CMS patients experience disruption in expressive language, emotional lability, loss of volitional movement, and a number of other symptoms during the early, acute phase of the disorder.<sup>1</sup> Speech function is regained in some capacity after a period of days to months, but some dysfunction of language, motor, and neurocognitive capabilities are commonly permanent.<sup>2,3</sup>

Reported rates in high-risk patients are currently 25%-35%.<sup>1,4</sup> The current understanding of CMS etiology is that surgical damage to the efferent cerebellar pathways is the principal cause,<sup>5,6</sup> as these structures constitute the primary neuronal output from the cerebellum toward the supratentorial brain. However, language impairment can result from damage to tissues “upstream” of the superior cerebellar peduncles as well, including the cerebellar nuclei and cortex. Furthermore, a recent study indicated that some areas of damage to the cerebellar outflow pathways cause mutism while others do not,<sup>5</sup> making it clear that specific cerebellar subsystems are responsible for CMS pathogenesis. Identification of these critical subsystems could help alter surgical strategies to reduce the risk of CMS. Furthermore, identification of the extracerebellar targets involved in this disorder would bolster our understanding of CMS and reveal new research opportunities and strategies for symptom mitigation.

Mb is the most prevalent and highest-risk cerebellar tumor leading to postoperative CMS. This embryonal tumor of the cerebellum is the most common childhood brain tumor, accounting for about 15% of brain tumors in children. Currently, approximately 20%-40% of all Mb resections result in complete mutism, while a greater percentage of patients experience at least a partial disruption of speech or an impairment of cognitive function.<sup>1,4</sup> Intraventricular Mb are overwhelmingly more likely to lead to postoperative CMS, apparently due to their proximity to the superior cerebellar peduncles and other critical neuronal structures that are at risk during extirpation of the tumor.

Here, we used a specially developed algorithm to map the surgical void in individual Mb patients to a standard space to investigate which surgical damage in high-risk

resection procedures contributes to mutism and speech impairment. We took three complementary approaches to analyze these maps: a voxel-wise approach that considers the contribution of each voxel to CMS outcome, a multivariate approach that considers the contribution of overall lesion pattern to CMS outcome, and a novel graph-pattern spatial analysis that identifies sets of voxels that uniquely correspond to CMS outcome when damage is contingent between them. Lastly, we used magnetization transfer imaging to measure focal histoarchitectural changes related to deafferentation (eg, Wallerian degeneration, demyelination) in cerebellar targets of the midbrain to investigate which cerebellar targets were selectively affected in CMS.

## Methods

### Patient Demographics and Diagnosis

Sequential postoperative MR imaging was acquired from 229 children and adolescents enrolled in a prospective study of patients undergoing treatment for Mb (SJMB12; NCT 01878617). All patients underwent a standardized postoperative neurological examination described in detail recently.<sup>1</sup> Based on the data from these examinations, diagnostic groups were defined to best represent the spectrum and clustering of symptoms within the cohort. This included two diagnostic groups which fall under the consensus definition of CMS,<sup>7,8</sup> differing primarily in the degree of speech disruption: “PFS1” characterized by complete mutism, and “PFS2” which was characterized by an abnormal paucity of speech (specifically, the inability to complete a 3-word sentence) (We preserve these group labels [PFS1 and PFS2] derived from the diagnostic term “Posterior Fossa Syndrome” to remain consistent with Khan et al.<sup>1</sup> Throughout the rest of this study, we use the terms “Cerebellar Mutism Syndrome” or CMS per the consensus definition put forth by the Posterior Fossa Society<sup>7,8</sup>). Further details regarding the patient cohort, examination schedule, clinical measures, and diagnostic criteria may be found in the precedent article by Khan et al.<sup>1</sup> Patients were excluded from further analysis if diagnosed with severe ataxia without CMS symptoms, or if diagnosed as asymptomatic following the resection of a non-intraventricular tumor, as these cases are known to be low risk for CMS<sup>4</sup> (Table 1). Imaging data at two timepoints

**Table 1.** Demographics of Mb Patients Used in Lesion Analyses and MTR Study

Diagnosis	Asymptomatic	PFS1 (Complete Mutism)	PFS2 (Partial Mutism)
Lesion analysis, n	85	47	20
MTR subset analysis, n	61	27	N/A
Age range (years)	3-22	3-20	3-18
Mean age (years)	8.98	7.62	7.45
Percent male	70.59	60.42	65.11

All listed subjects presented with midline intraventricular Mb considered high risk for CMS.

were evaluated for surgical damage: the initial postoperative imaging that occurred within 2 weeks of surgery, and the first follow-up, which was approximately 3 months of post-surgery after the completion of radiation therapy. Ultimately, image data from 84 asymptomatic, 34 PFS1, and 18 PFS2 patients were analyzed for the first timepoint in the current study, while 85 asymptomatic, 47 PFS1, and 20 PFS2 patients were analyzed for the second timepoint.

### Image Acquisition

3DT1 images were used in the analysis of lesion location (sagittal MPRAGE sequence, TR/TE 1980/2.26 ms, 1.0 mm pixel space, 256 × 256 matrix, 160 slices, 1.0 mm slice thickness). Patients were imaged at up to five timepoints between 1 day and 21 months following tumor resection. An early examination of images taken at various timepoints indicated that they may offer different information about surgical damage, as the surgical corridor is more apparent in early postoperative imaging while the extent of tissue loss in periventricular parenchyma is more apparent in later imaging after edema and other reactive postoperative changes subside. Additionally, 13 subjects with CMS were excluded from the analysis of the initial postoperative imaging due to obscuring factors that resolved in follow-up imaging, such as the appearance of abundant blood degradation product or hemostatic surgical dressing. Thus, we chose to analyze images from two timepoints for the location of surgical damage (see above) in order to glean the most information from the available data.

Magnetization transfer ratio (MTR) images were examined for evidence of neuronal circuit disruption in downstream targets of the cerebellum in the PFS1 cohort. These images were acquired at 1.0 and 1.5 years postoperative time with a bSSFP-MT sequence (TR/TE 4.39/2.2 ms for  $M_{\min}$ , 3.09/1.55 ms for  $M_{\text{sat}}$ ,  $\alpha = 30^\circ$ ; 3.5 minutes) and MTR images were calculated as  $100 \times (M_{\min} - M_{\text{sat}}) / M_{\min}$ . These later timepoints were chosen as they would allow sufficient time for indication of neuronal disruption to occur,<sup>9,10</sup> while allowing reactive changes to subside. Region-of-interest (ROI) MTR values were averaged between the two timepoints for each subject.

### Normalization and Lesion Detection

Full technical description of the cerebellar normalization and lesion detection has been described in detail

elsewhere (<https://doi.org/10.48550/arXiv.2203.02042>). In brief, gray and white matter segmentation was performed on the 3DT1 image in native space, and the cerebellum and brainstem were isolated using a combination of custom tools and SUIT (spatially unbiased intracranial toolbox) cerebellum templates (Figure 1), which were developed for normalization of cerebellar anatomy with improved performance over whole-brain normalization techniques.<sup>11</sup> Then, a non-linear transformation to SUIT space was performed using anatomical information derived from the gray and white matter segmentation. Resected or lesioned tissue was then detected by comparison to the cerebellar template. The resulting lesion map was then verified by an expert in cerebellar anatomy and a neuroradiologist blinded to the diagnosis before further analysis. If lesion detection was determined to have failed, then the lesion mask was manually edited before repeating the verification process.

### Voxel-wise Lesion Analyses

To identify regions where surgical damage shows an association with CMS, the lesion maps for the diagnostic groups were contrasted on a voxel-wise basis. Lesion maps for the diagnostic groups were created by summation across their subjects. Voxels with statistically significant incidence of damage in CMS vs the control (asymptomatic) were identified using a Monte Carlo hypothesis test; diagnoses were randomized 10 000 times and voxels were highlighted which had higher incidence of damage in the PFS1 or PFS2 groups than expected ( $P < .001$ ). Lesion areas were also identified as unique to CMS if damage occurred at a given voxel exclusively in PFS1 or PFS2 cases.

### Lesion-Symptom Mapping

Multivariate lesion-symptom mapping was performed for comparison to recent study.<sup>5</sup> Support vector machines were used to create a beta map in Matlab (command `fitcsvm.m`) modeling the relationship between lesion location and CMS outcome. A 4-fold cross-validation was performed to calculate the correlation between predicted and actual diagnoses. Due to the relatively low number of subjects with a PFS2 diagnosis, LSM was only performed on the PFS1 subjects in contrast with the asymptomatic group.

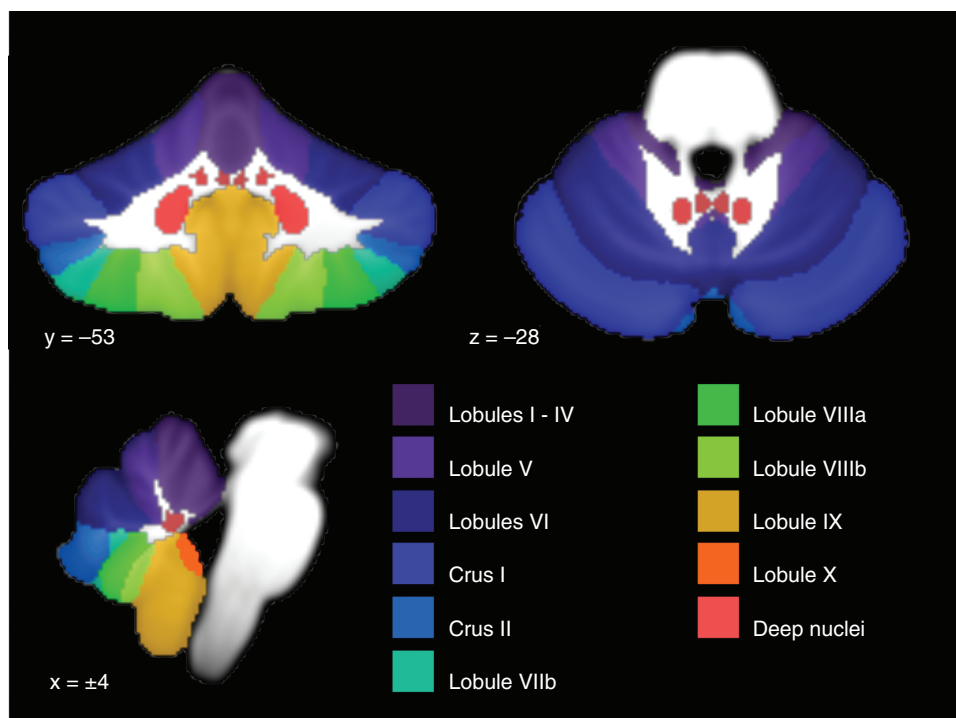


**Fig. 1** Anatomical reference atlas for cerebellar cortical lobules and deep cerebellar nuclei (medial to lateral: fastigial, interposed, and dentate nuclei).

### Graph-Pattern Lesion Analysis

To help identify multivoxel patterns of surgical damage unique to patients with mutism, a novel graph network analysis was developed to determine whether specific pairs of voxels were connected by a contiguous lesion volume. This would determine, for example, whether CMS symptoms were contingent upon damage spanning a certain white matter tract or cerebellar lobule when partial damage to the structures may not produce CMS symptoms.

To test this, logical matrices were generated from the lesion maps to represent which pairs of voxels within the 3D space were connected by a contiguous lesion. The matrix space was reduced to represent only the voxels that overlapped between the PFS1 and asymptomatic groups, as any pair containing a uniquely damaged voxel in the PFS1 group would also be unique. Lesion maps were generated for each subject in Matlab ( $n_{\text{voxel}} \times n_{\text{voxel}}$  logical matrix, lesion contiguity determined by 26-connected adjacency using command `bwconncomp.m`), and then summed across subjects to create group matrices. CMS-unique voxel pairs were identified by eliminating values in the PFS1 group matrices from positions where one or more asymptomatic subjects had equivalent damage.

These results were projected back to the 3D space for visualization in two ways. First, the matrices were summed across one dimension to give the total number of CMS-unique damage pairs associated with each voxel as an endpoint for the given subject. Group maps were created

using weighted summation across subjects by dividing the total number of pairs at each voxel by the number of possible pairs for each subject based on lesion size, and then adding these values across subjects. These values were then tested for significance using the same resampling procedure as for the voxel-wise damage analysis to find which voxels were frequently involved in unique damage patterns associated with CMS. Secondly, damage patterns associated with these statistically significant voxels were reconstituted by finding the shortest path between pairs of voxels through the lesion space. The resulting image represents how many times a CMS-unique lesion path passed through each voxel, with greater emphasis on smaller lesion spaces associated with CMS.

### MTR Analysis

MTR images from the PFS1 and asymptomatic patients were analyzed for evidence of neuronal circuit disruption in efferent targets of the cerebellum in subjects with mutism. Images from PFS2 subjects were not analyzed due to insufficient data from this group, as well as a lack of a strong rationale as these subjects did not show significant cerebellar nuclear or efferent pathway damage. Whole-brain MTR images were spatially normalized using SPM12 (University College London, <http://www.fil.ion.ucl.ac.uk/spm>). MTR values for the red nuclei, periaqueductal gray (PAG), and reticular formation were selected a priori as potentially relevant axonal targets of the cerebellar nuclei. Values were

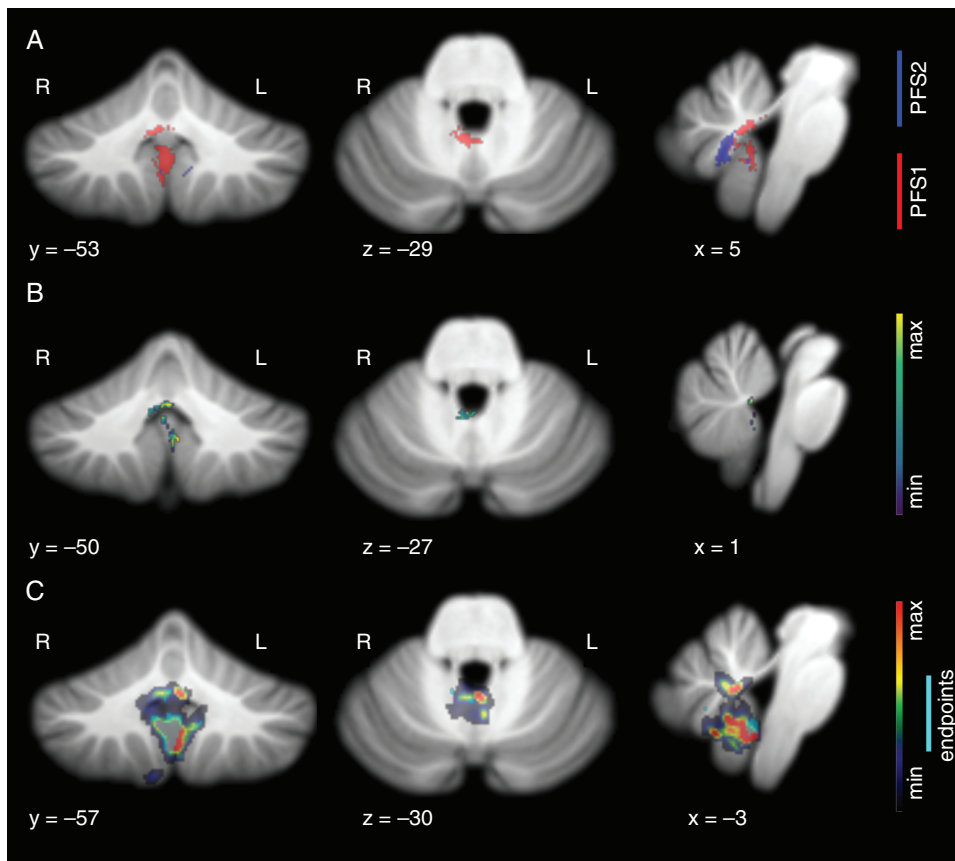


**Fig. 2** Lesion patterns observed in speech-impaired subjects at initial postoperative imaging. (A) Voxel-wise results show significant incidence of damage in the right fastigial nucleus, proximal superior cerebellar peduncles, and inferior vermis in subjects with complete mutism ( $P < .001$ ). Subjects with paucity of speech showed damage in right vermal lobule VIIIb, in gray and white matter proximal to the fastigial nucleus ( $P < .001$ ). (B) Result of lesion-symptom mapping. Voxel color represents positive association with PFS1 diagnosis, with peak finding at the cerebellar commissure, where output tracts from bilateral fastigial nuclei decussate. Additional peak is present at left lobule IX. (C) Result of graph-pattern analysis showing significant involvement of the right fastigial nucleus as a damage endpoint and left fastigial nucleus as contingent damage for CMS-unique lesion patterns. Inferior vermis and bilateral lobule IX also showed significant incidence in CMS-unique damage.

calculated as the mean of the MTR values within the corresponding ROIs, using a standard atlas resampled into the MTR space.<sup>12</sup> ROI accuracy was verified by visual inspection for each image prior to analysis. Voxels from the dorsal portion of the PAG were eliminated from the PAG ROI while the ventral and lateral portions were preserved. This was done for two reasons: first, the ventral and lateral portions of the PAG are thought to receive the majority of input from the cerebellar nuclei,<sup>13,14</sup> and second, variability in the diameter of the cerebral aqueduct (eg, due to prior hydrocephalus) contributed to distortion of the dorsal PAG. Voxels in the PAG ROI which showed overlap with the cerebral aqueduct were manually removed in each subject by experimentors blinded to diagnosis to prevent anatomical variance from affecting the MTR average.

## Results

For ease of interpretation, the results of all analyses for the initial postoperative imaging timepoint (Figure 2) and

the follow-up imaging timepoint (Figure 3) are presented together.

### Voxel-wise Lesion Analyses

The voxel-wise analysis demonstrated that both PFS1 and PFS2 groups had significantly different damage profiles than asymptomatic controls. Furthermore, the significant surgical damage patterns in these two groups had little overlap, suggesting that this analysis effectively highlights a potential difference in the anatomical substrate of observed symptoms in these two groups (Figure 2A). Patients diagnosed as PFS1 had significantly higher incidence of damage to the right proximal efferent cerebellar pathway, putative location of the right fastigial nucleus (FN), the cerebellar commissure, and vermal lobule IX. PFS2 patients had significantly higher incidence of damage on the right half of vermal lobule VIII. The anterior aspect of the PFS2 pattern did overlap with the posterior aspect of the PFS1 pattern in initial postoperative images, centered approximately on the right white matter efferent of vermal lobule

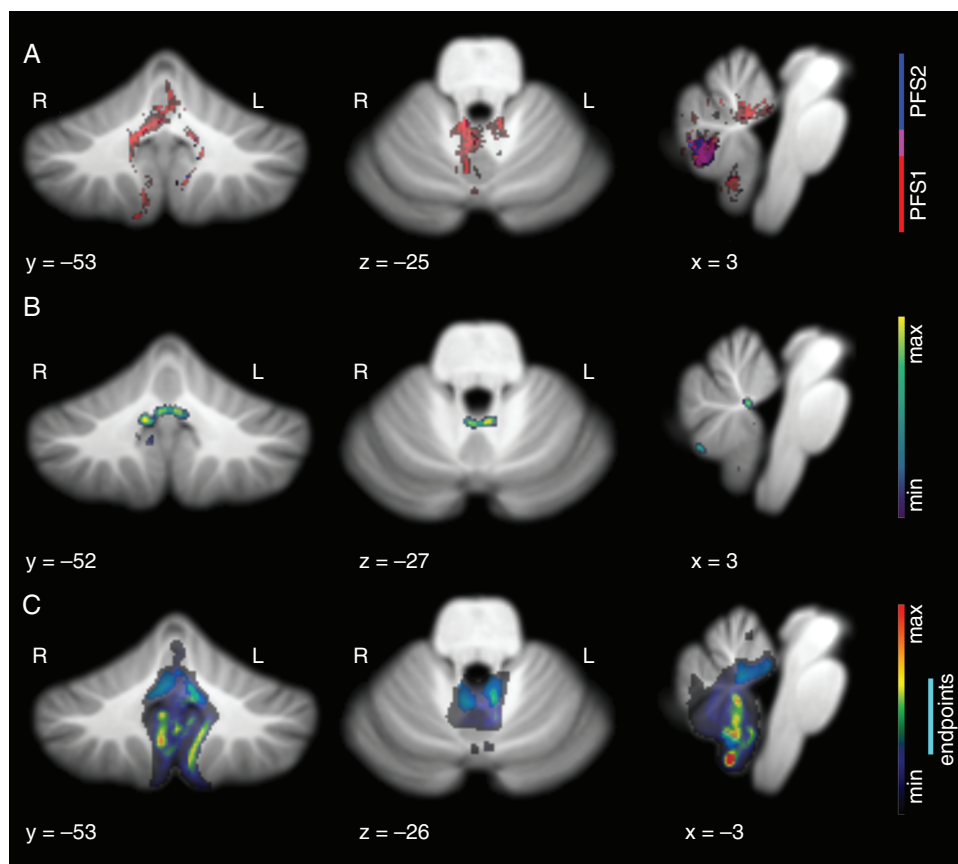


**Fig. 3** Lesion patterns observed in speech-impaired subjects at follow-up imaging >3-month postoperative time. (A) Voxel-wise results show the most significant incidence of damage in the right fastigial nucleus, bilateral proximal superior cerebellar peduncles, and right vermal lobule VIIIb in subjects with complete mutism ( $P < .001$ ). Subjects with paucity of speech showed damage in right vermal lobule VIIIb overlapping with that of CMS subjects ( $P < .05$ ). (B) Results of lesion-symptom mapping show clear peak findings in the bilateral fastigial nuclei and right interposed nucleus. (C) Result of graph-pattern analysis showing significant involvement of fastigial nuclei bilaterally as damage endpoints. Contingent damage for CMS-unique lesion patterns peaked in the area of the left fastigial nucleus and proximal superior cerebellar peduncle, the inferior vermis, and bilateral lobule IX.

VIII. This may be a transition point where damage nearing the cerebellar nuclei and their converging inputs results in greater impairment. Analysis of the second timepoint showed a greater degree of overlap in the lesion space located at the right posterior aspect of vermal lobule VIII.

Despite similar tumor locations in both CMS and asymptomatic patients, surgical damage from the right posterior area of vermal lobule VIII only occurred in the CMS subjects (PFS1 and PFS2), according to the initial postoperative imaging. This was the location with the highest incidence of CMS-unique damage, with up to 30.8% of patients in both CMS groups incurring surgical damage to this slightly off-midline area in initial postoperative imaging (Figure 4). Damage to the superior-lateral face of the right superior cerebellar peduncle was unique to the PFS1 group, with 11.7% of PFS1 patients showing damage here. Destruction of the superior-lateral face represents a complete transection of the tract, given that the surgical site originates within the fourth ventricle. Additionally, 11.7% of PFS1 patients showed damage overlapping in the area of

the right anterior dentate nucleus, where no asymptomatic or PFS2 subject showed damage.

### Lesion-Symptom Mapping

Lesion-symptom mapping was performed to determine whether an overall lesion pattern was predictive of clinical symptoms and to make a comparison to a recent study using a similar multivariate approach.<sup>5</sup> Our model found a significant relationship between lesion pattern and CMS diagnosis ( $r = 0.3556/P = .00024427$  for initial postoperative images,  $r = 0.4656/P < .10$  for follow-up images). In initial postoperative imaging, peak findings were along the anteromedial face of left vermal lobule IX, and the anterior portion of the cerebellar commissure (Figure 2B). Smoothing of the beta map revealed a broader peak in the area of the right FN and proximal superior cerebellar peduncle, in alignment with findings from the voxel-wise approach. In follow-up images, peak findings were in the FNs bilaterally, and the right interposed nucleus (Figure 3B).

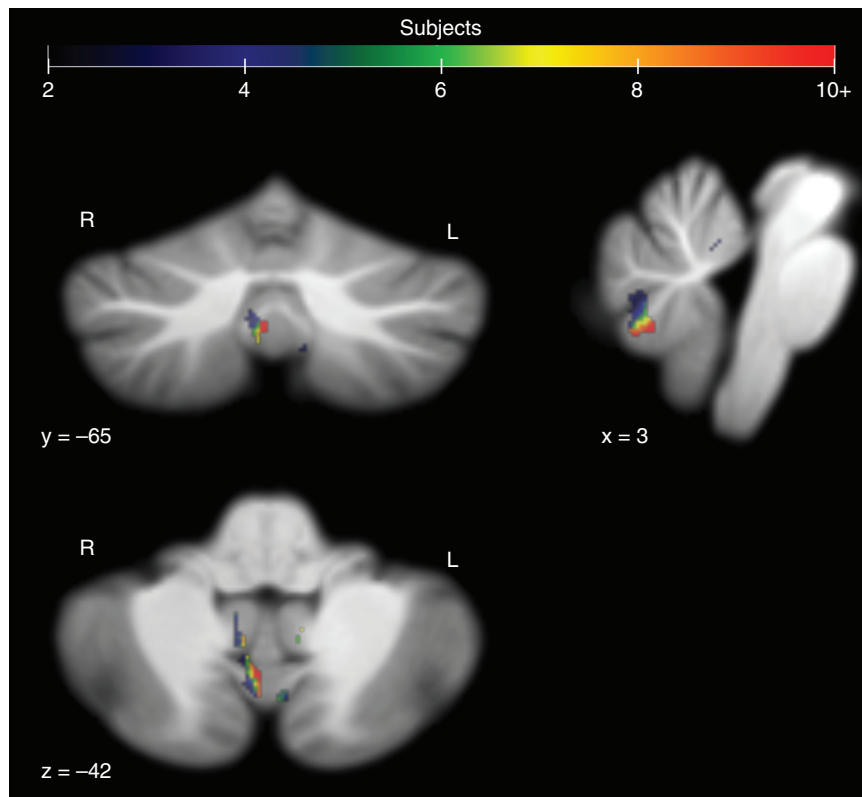


**Fig. 4** Voxels containing surgical damage in CMS subjects (PFS1 and PFS2) that did not appear in any asymptomatic subjects at the initial postoperative image session. Damage occurred in 16 of the 52 combined CMS subjects at the listed coordinates for the right side of vermal lobule VIIIa.

### Graph-Pattern Lesion Analysis

Damage leading to CMS can be variable, even within the normalized space. Thus, to identify areas consistently involved in patterns of damage associated with CMS, we visualized the voxels linked to CMS-unique damage at a significant frequency as endpoints in a contiguous damage path. PFS1 patients showed unique damage originating from the right inferior FN, right superior cerebellar peduncle, right lobule I-IV, vermal lobule VIII, and both vermal and lateral regions of lobule IX (Figure 2C). Visualization of the shortest paths associated with these endpoints revealed additional involvement of the left FN and cerebellar commissure. Peak findings for the shortest paths were found in the inferior vermis to the right side of lobules VIII and IX. In follow-up imaging, endpoints encompass the fastigial nuclei bilaterally and extend into the superior cerebellar peduncle on the left. Contingent damage for these endpoints extends predominantly into the inferior vermis as well as lobule IX, bilaterally.

### MTR Changes in CMS Subjects

Magnetization transfer imaging was used to identify long-term parenchymal tissue matrix changes in PFS1 subjects occurring downstream of the cerebellum. At 1.0 and

1.5 years postoperative time, MTR values in the ventral PAG were significantly lower in PFS1 subjects compared to controls ( $P = .0002$ ), implicating this region as a likely axonal target of critical cerebellar structures involved in CMS etiology (Figure 5). Bilateral red nuclei showed significant decrease in MTR values in CMS subjects relative to asymptomatic subjects, with the left red nucleus showing more consistent differences than the right ( $P < .0001$  vs  $P = .0156$ , respectively). In contrast, the reticular formation showed no difference in MTR value between diagnostic groups ( $P = .2411$ ).

## Discussion

This study, to the best of our knowledge, is the largest lesion-mapping study examining CMS outcomes in patients with high-risk intraventricular Mb. Our findings broadly support conclusions made in a recent study contrasting cerebellar cognitive-affective syndrome with CMS<sup>5</sup>: that the FNs, inferior vermal lobules, and cerebellar outflow pathways are critical regions implicated in the pathogenesis of CMS. Furthermore, we affirm that these results reflect the involvement of a cerebellar circuit, within which certain areas may have a more detrimental effect on circuit function and output, resulting in the markedly

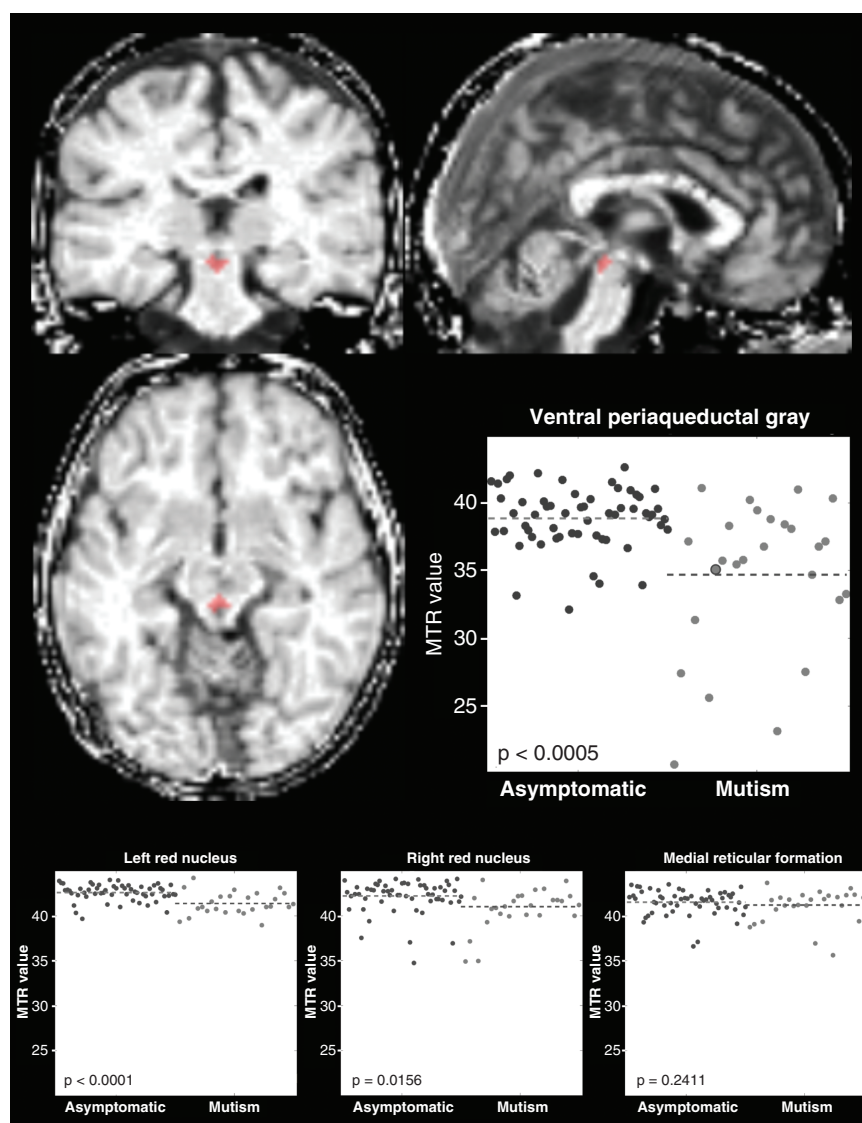


**Fig. 5** Late (>1 year) postoperative differences in magnetization transfer ratio of anatomical targets of cerebellar output. Normalized whole-brain MTR image shows an example ventral PAG ROI in red for an individual subject with postoperative CMS. Scatterplots show MTR values for individual subjects both asymptomatic (dark gray) and with CMS (light gray; large dot in the ventral PAG plot represents MTR value of the example subject). Decreased MTR values in CMS suggest demyelination as a feature of CMS, likely due to surgical injury of afferent fibers in the cerebellum, or secondary cell injury caused by excitotoxicity. Significant decrease in MTR was observed in the ventral PAG and the red nuclei bilaterally, although group differences were more consistent within the left red nucleus. No CMS-related difference in MTR was observed in the medial reticular formation.

different degrees of speech impairment we see in patients with complete (PFS1) vs partial mutism (PFS2).

This study is also, to the best of our knowledge, the first to provide a direct link between PAG disruption and CMS pathogenesis in humans. As such, the implications of this finding warrant robust discussion. Collectively, our results support the hypothesis that some CMS symptoms, such as persistent linguistic/metalinguistic impairment and disruption of normal neurocognitive development, result from a loss of feedback from the cerebellum to the supratentorial brain.<sup>15–17</sup> However, the “core” CMS

symptoms characterized by volitional impairment like mutism and apraxia may constitute a distinct cluster of symptoms with a separate cause: the destruction of cerebellar output to nuclei in the midbrain PAG responsible for the gating of complex behaviors like vocalization and voluntary movement.<sup>18–20</sup> The functions subserved by the PAG align closely with the core deficits seen in CMS, including mutism, apraxia, opsoclonus, irritability, and dysphagia.<sup>1,14,20</sup> The rate of apraxia is twice as high in patients with complete mutism than partial mutism (80% in PFS1 vs 40% in PFS2), and is nonexistent in subjects without



postoperative speech impairment, in our experience.<sup>1</sup> This strongly suggests a common underlying mechanism for these symptoms. We believe the critical cerebellar outflow fibers for these PAG-mediated functions originate in the FNs and, to a lesser extent, in the interposed nuclei and anterior dentate as is supported by human imaging,<sup>13</sup> making damage to these areas particularly devastating. Importantly, the ascending uncinate tracts emanating from the inferior FNs decussate in the anterior portion of the cerebellar commissure, a region that was highlighted in all of our analyses. Damage in this area may be especially subtle but devastating, as tissue missing along the posterior limit of the fourth ventricle would be difficult to visually detect but could effectively destroy output from bilateral inferior FNs.

Recent studies in rodents have separately established bilateral FN lesions as a valid animal model for CMS<sup>21</sup> and revealed that projections to PAG can gate complex behaviors in a way that mimics CMS symptoms. Transient excitement of specific terminals in PAG is sufficient to halt movement and/or socially oriented vocalization entirely.<sup>22–24</sup> The gating of body movement is a primitive function essential for evading the notice of nearby predators,<sup>20</sup> and cerebellar output to PAG is known to play a role in triggering this “freezing” behavior.<sup>19,20</sup> The role of the cerebellum in freezing was demonstrated recently by optical activation of projections from the FNs to the ventrolateral PAG, resulting in sudden and sustained immobility for the duration of the stimulation.<sup>24</sup> Gating of vocalization appears more complicated, with both positive and negative sources of influence on PAG.<sup>23,25</sup> For example, vocalization can be elicited via activation of hypothalamic projections to the lateral PAG, while projections from the amygdala suppress vocalization.<sup>22</sup> Optical stimulation of the lateral PAG itself can evoke vocalization, but only during certain phases of the respiratory cycle.<sup>23</sup> Synaptic silencing of vocalization-related neurons in the PAG left most of the mice completely mute, with all mice showing a dramatic reduction in vocalization.<sup>23</sup> Similar impairment of social vocalization was observed in rats with bilateral FN lesioning, which was recovered over a period of weeks.<sup>21</sup> While the functional role of specific FN projections to PAG has not been directly explored with respect to mutism, there are two known pathways from the FNs to the vocalization center of the PAG: the direct pathway from FN to PAG, and an indirect pathway via the parafascicular thalamic nucleus and amygdala.<sup>14,26</sup> These examples show that destruction of the fastigial nuclei or a change in synaptic input to specific domains of the PAG can result in the suppression of complex behaviors that mimic the characteristics of CMS. Future animal studies could clarify the effect of FN output on vocalization and determine whether the FN influences PAG indirectly via the amygdala, or directly as our imaging data suggest.

The indirect impact that these surgeries have on PAG function may help explain why mutism and apraxia are transient, and why some patients experience a delayed onset of symptoms of up to several days. Direct incidental lesioning of the PAG is extremely rare but has been reported to cause irreversible mutism in the case of stroke.<sup>27</sup> Specific experimental lesioning of the PAG has also been shown to cause irreversible mutism and akinesia in cats,<sup>28</sup>

dogs,<sup>29</sup> and monkeys.<sup>30</sup> In cases of CMS, destruction of cerebellar output may result in an indirect (and potentially delayed or accumulating) disruption of PAG neuronal function lasting until sufficient function can be regained to allow the initiation of speech once again. The compensatory mechanism for this restitution of function remains unknown, but understanding which processes lead to the restoration of PAG function could offer new avenues for intervention and treatment. Our results also show that lesions further upstream of the PAG resulted in less severe symptoms, with pre-fastigial vermal and paravermal tissue damage leading to partial rather than complete mutism. This suggests that disruption of input to the FNs has a noticeable but less severe impact on speech function than the loss of FN output altogether. This gradation in the severity of speech impairment as lesions occur further upstream of the PAG is consistent with its expected role in the gating of speech.<sup>18</sup>

The PAG also provides feedback to the cerebellum which may exacerbate the disruption of other cerebellar subsystems, including those which project to the cerebral cortex via the red nuclei. Descending output from the PAG also plays a role in the modulation of sensory responses occurring within the cerebellum, via the olivo-cerebellar pathway.<sup>31</sup> Stimulation of PAG neurons *in vivo* results in suppression of neuronal responses in FN to nociceptive input.<sup>31</sup> Functionally, this pathway underlies passive coping strategies for discomfort, and the regulation of emotional defensive behaviors,<sup>32</sup> including suppression of movement and vocalization. It's evinced from these findings that the FN and PAG form a neuronal circuit with self-regulating properties, with PAG providing negative feedback via the inferior olive when given excitatory input from FN. It remains to be examined how disruption of this circuit could affect the function of ancillary structures and circuits, including the dentato-rubro-olivary circuitry that shows clear signs of dysfunction and degeneration in this and other studies.<sup>33,34</sup> The overlapping structure and complementary function of these circuits undoubtedly make their individual contribution to CMS difficult to discern.

Our lesion analyses additionally highlighted portions of the posterior cerebellum, including lobules IX bilaterally, vermal lobule X, and a region of vermal lobule VIII. Surgical damage to the right half of vermal lobule VIII was the only distinguishing feature of patients with partial mutism, suggesting an important role for this structure in CMS pathogenesis. This region projects heavily to the FN and is functionally linked to limbic areas of the cerebrum involved in speech initiation and emotional regulation.<sup>35,36</sup> Lobule IX and X damage in patients with complete mutism was a notable feature in the analyses of initial postoperative imaging but did not remain apparent in later imaging. This might reflect long-term structural changes surrounding the surgical area (eg, atrophy) which could be common to both groups over that duration. The initial finding may also reflect a tendency for CMS-associated tumors to be large and invasive,<sup>37</sup> which could explain the highlighted volume in the inferior cerebellum by the graph-pattern analysis (Figure 2C, red area). Still, the possibility remains that lobule IX damage contributes to CMS symptoms. Importantly, lobule IX is in some ways more closely

aligned functionally with vermal regions than hemispheric regions of the anterior cerebellum,<sup>35,36</sup> with an apparent role in language and emotional processing.<sup>38,39</sup>

The focus of this study was on the impact of tissue that is resected, leading to certain and permanent ablation of function for the involved area. This approach is concrete but conservative, as surgical injury may disrupt the function of various structures without their complete resection. These surgical injuries may lead to the appearance of necrosis, rarefaction, or other imaging features that could be considered in future studies. Excessive and prolonged manipulation of the normal structures around a fourth ventricular mass may contribute to unaccounted tissue damage that may contribute to CMS.

Preoperative factors affecting risk for CMS are yet unaddressed since we focused on patients with a high level of preoperative risk. The predominance of different molecular subtypes of Mb in different stages of life, and how this contributes to tumor location and surgical risk, tends to confound the relationship between age and CMS. In the precedent study of all Mb patients, age was a significant contributor to risk<sup>1</sup> (age-related odds ratio for PFS1 or PFS2 = 0.81,  $P = .0005$ ). This relationship was largely diminished within the intraventricular cases herein (odds ratio = 0.93,  $P = .0568$ ). Whether any remaining trend may reflect changing predisposition to CMS with development or an impact of age on the difficulty of safe surgery remains to be determined.

Lastly, a key finding was that off-midline damage to the right inferior vermis was relatively common in subjects with speech impairment but did not occur in any asymptomatic subjects (Figure 4). It remains unclear whether damage to these tissues is a driving factor for speech impairment, or whether it may serve as proxy for other factors affecting patient risk, such as surgeon handedness, patient position, tumor grade, or surgical approach.<sup>37</sup> Notably, a recent study found no clear association between surgical approach and CMS for high-risk tumors like those herein,<sup>40</sup> although laterality of approach was not denoted. Data relating surgical techniques to lesion location will be needed in future studies to resolve this question.

## Keywords

cerebellar mutism syndrome | fastigial nuclei | medulloblastoma | periaqueductal gray | posterior fossa syndrome

## Ethical Approval

The protocol was approved by the St Jude Institutional Review Board and was performed in accordance with the ethical standards of the institution and with the 1964 Helsinki Declaration and its later amendments or comparable ethical standards. All patients and/or their legal guardians provided written informed consent prior to participation in the study.

## Funding

This work was supported by the American Lebanese Syrian Associated Charities (ALSAC).

**Conflict of interest statement.** None to declare.

**Authorship statement.** Study design: S.S.M. and M.A.S. Clinical trial: A.G., G.R., and Z.P. Development of diagnostic criteria: R.K., H.M.C., and D.R. Lesion analyses: S.Z., S.S.M., and M.A.S. Lesion map review: Z.P. MTR analysis: S.S.M. and P.Z. Surgical interpretation: P.K. Writing: S.S.M. Editing: S.S.M. and M.A.S.

## References

1. Khan RB, Patay Z, Klimo P, et al. Clinical features, neurologic recovery, and risk factors of post-operative posterior fossa syndrome and delayed recovery: a prospective study. *Neuro Oncol.* 2021;23(9):1586–1596.
2. Doxey D, Bruce D, Sklar F, Swift D, Shapiro K. Posterior fossa syndrome: identifiable risk factors and irreversible complications. *Pediatr Neurosurg.* 1999;31(3):131–136.
3. Paquier PF, Walsh KS, Docking KM, et al. Post-operative cerebellar mutism syndrome: rehabilitation issues. *Childs Nerv Syst.* 2020;36(6):1215–1222.
4. Turgut M. Cerebellar mutism. *J Neurosurg Pediatr.* 2008;1(3):262.
5. Albazon FM, Bruss J, Jones RM, et al. Pediatric postoperative cerebellar cognitive affective syndrome follows outflow pathway lesions. *Neurology.* 2019;93(16):e1561–e1571.
6. Catsman-Berrevoets C, Patay Z. Cerebellar mutism syndrome. *Handb Clin Neurol.* 2018;155:273–288.
7. Gudrunardottir T, Morgan AT, Lux AL, et al. Consensus paper on post-operative pediatric cerebellar mutism syndrome: the Iceland Delphi results. *Childs Nerv Syst.* 2016;32(7):1195–1203.
8. Molinari E, Pizer B, Catsman-Berrevoets C, et al. Posterior Fossa Society Consensus Meeting 2018: a synopsis. *Childs Nerv Syst.* 2020;36(6):1145–1151.
9. Goyal M, Versnick E, Tuite P, et al. Hypertrophic olivary degeneration: metaanalysis of the temporal evolution of MR findings. *AJNR Am J Neuroradiol.* 2000;21(6):1073–1077.
10. Thomalla G, Glauche V, Weiller C, Rother J. Time course of Wallerian degeneration after ischaemic stroke revealed by diffusion tensor imaging. *J Neurol Neurosurg Psychiatry.* 2005;76(2):266–268.
11. Diedrichsen J. A spatially unbiased atlas template of the human cerebellum. *Neuroimage.* 2006;33(1):127–138.
12. Keuken MC, Forstmann BU. A probabilistic atlas of the basal ganglia using 7 T MRI. *Data Brief.* 2015;4:577–582.
13. Cacciola A, Bertino S, Basile GA, et al. Mapping the structural connectivity between the periaqueductal gray and the cerebellum in humans. *Brain Struct Funct.* 2019;224(6):2153–2165.
14. Fujita H, Kodama T, du Lac S. Modular output circuits of the fastigial nucleus for diverse motor and nonmotor functions of the cerebellar vermis. *eLife.* 2020;9:e58613.

15. Argyropoulos GPD, van Dun K, Adamaszek M, et al. The cerebellar cognitive affective/Schmahmann syndrome: a Task Force Paper. *Cerebellum*. 2020;19(1):102–125.
16. McAfee SS, Liu Y, Sillitoe RV, Heck DH. Cerebellar coordination of neuronal communication in cerebral cortex. *Front Syst Neurosci*. 2021;15:781527.
17. Schmahmann JD. The cerebellum and cognition. *Neurosci Lett*. 2019;688:62–75.
18. Holstege G, Subramanian HH. Two different motor systems are needed to generate human speech. *J Comp Neurol*. 2016;524(8):1558–1577.
19. Koutsikou S, Crook JJ, Earl EV, et al. Neural substrates underlying fear-evoked freezing: the periaqueductal grey-cerebellar link. *J Physiol*. 2014;592(10):2197–2213.
20. Watson TC, Koutsikou S, Cerminara NL, et al. The olivo-cerebellar system and its relationship to survival circuits. *Front Neural Circuits*. 2013;7:72.
21. Al-Afif S, Krauss JK, Helms F, et al. Long-term impairment of social behavior, vocalizations and motor activity induced by bilateral lesions of the fastigial nucleus in juvenile rats. *Brain Struct Funct*. 2019;224(5):1739–1751.
22. Michael V, Goffinet J, Pearson J, et al. Circuit and synaptic organization of forebrain-to-midbrain pathways that promote and suppress vocalization. *eLife*. 2020;9:e63493.
23. Tschida K, Michael V, Takatoh J, et al. A specialized neural circuit gates social vocalizations in the mouse. *Neuron*. 2019;103(3):459–472.e4.
24. Vaaga CE, Brown ST, Raman IM. Cerebellar modulation of synaptic input to freezing-related neurons in the periaqueductal gray. *eLife*. 2020;9:e54302.
25. Zhang SP, Davis PJ, Bandler R, Carrive P. Brain stem integration of vocalization: role of the midbrain periaqueductal gray. *J Neurophysiol*. 1994;72(3):1337–1356.
26. Frontera JL, Baba Aissa H, Sala RW, et al. Bidirectional control of fear memories by cerebellar neurons projecting to the ventrolateral periaqueductal grey. *Nat Commun*. 2020;11(1):5207.
27. Esposito A, Demeurisse G, Alberti B, Fabbro F. Complete mutism after midbrain periaqueductal gray lesion. *Neuroreport*. 1999;10(4):681–685.
28. Adametz J, O’Leary JL. Experimental mutism resulting from periaqueductal lesions in cats. *Neurology*. 1959;9:636–642.
29. Skultety FM. Experimental mutism following electrolytic lesions of the periaqueductal gray matter in dogs. *Trans Am Neurol Assoc*. 1961;86:245–246.
30. Bailey P, Davis EW. Effects of lesions of the periaqueductal gray matter on the *Macaca mulatta*. *J Neuropathol Exp Neurol*. 1944;3(1):69–72.
31. Koutsikou S, Watson TC, Crook JJ, et al. The periaqueductal gray orchestrates sensory and motor circuits at multiple levels of the neuraxis. *J Neurosci*. 2015;35(42):14132–14147.
32. Koutsikou S, Apps R, Lumb BM. Top down control of spinal sensorimotor circuits essential for survival. *J Physiol*. 2017;595(13):4151–4158.
33. Avula S, Spiteri M, Kumar R, et al. Post-operative pediatric cerebellar mutism syndrome and its association with hypertrophic olivary degeneration. *Quant Imaging Med Surg*. 2016;6(5):535–544.
34. Patay Z, Enterkin J, Harreld JH, et al. MR imaging evaluation of inferior olivary nuclei: comparison of postoperative subjects with and without posterior fossa syndrome. *AJNR Am J Neuroradiol*. 2014;35(4):797–802.
35. Sang L, Qin W, Liu Y, et al. Resting-state functional connectivity of the vermal and hemispheric subregions of the cerebellum with both the cerebral cortical networks and subcortical structures. *Neuroimage*. 2012;61(4):1213–1225.
36. Stoodley CJ, Schmahmann JD. Evidence for topographic organization in the cerebellum of motor control versus cognitive and affective processing. *Cortex*. 2010;46(7):831–844.
37. Cobourm K, Marayati F, Tsering D, et al. Cerebellar mutism syndrome: current approaches to minimize risk for CMS. *Childs Nerv Syst*. 2020;36(6):1171–1179.
38. Baumann O, Mattingley JB. Functional topography of primary emotion processing in the human cerebellum. *Neuroimage*. 2012;61(4):805–811.
39. Guell X, Gabrieli JDE, Schmahmann JD. Triple representation of language, working memory, social and emotion processing in the cerebellum: convergent evidence from task and seed-based resting-state fMRI analyses in a single large cohort. *Neuroimage*. 2018;172:437–449.
40. Gronbaek JK, Wibroe M, Toescu S, et al. Postoperative speech impairment and surgical approach to posterior fossa tumours in children: a prospective European multicentre cohort study. *Lancet Child Adolesc Health*. 2021;5(11):814–824.